Journal of Materials Science Research; Vol. 12, No. 1; 2023
ISSN 1927-0585 E-ISSN 1927-0593
Published by Canadian Center of Science and Education

Characterization of Clay Materials from Côte d'Ivoire: Possible Application for the Electrochemical Analysis

Ségnéninhinténin Bakary Soro[1,2], Mariame Coulibaly[2], Legré Paul Gauly[1,2]
Seiny Roger N'Dri[2], Ali Sanou[2,3] & Albert Trokourey[1]

[1] Laboratoire de Constitution et Réaction de la Matière, Université Félix Houphouët-Boigny, 22 BP 582 Abidjan, Côte d'Ivoire

[2] Laboratoire des Sciences Physiques Fondamentales et Appliquées, Ecole Normale Supérieure d'Abidjan, 08 BP 10 Abidjan, Côte d'Ivoire

[3] Laboratoire des Procédés Industriels de Synthèses de l'Environnement et des Energies Nouvelles Institut National Polytechnique Félix Houphouët-Boigny, BP 1313 Yamoussoukro, Côte d'Ivoire

Correspondence: Mariame Coulibaly, Laboratoire des Sciences Physiques Fondamentales et Appliquées, Ecole Normale Supérieure d'Abidjan, 08 BP 10 Abidjan, Côte d'Ivoire. Email: coulibaly.mariame@ensabj.ci

Received: April 3, 2023 Accepted: May 14, 2023 Online Published: May 25, 2023

doi:10.5539/jmsr.v12n1p51 URL: https://doi.org/10.5539/jmsr.v12n1p51

Abstract

The utilization of clay minerals as electrode modifiers is based on their unique structure and properties. In this study, clays from various regions of Côte d'Ivoire were characterized for their potential use in developing electrochemical sensors. The clay samples underwent analysis via X-ray diffraction (XRD), scanning electron microscopy (SEM), energy-dispersive X-ray spectroscopy (EDS) mapping analysis, Fourier transform infrared spectroscopy (FTIR), and X-ray fluorescence (XRF). Results from XRD, FTIR, SEM, and XRF indicated that kaolinite was the primary component mineral phase in all samples. These clays were then employed as modifying agents to prepare modified carbon paste electrodes, and the electrochemical behavior of ferri/ferrocyanide was studied via cyclic voltammetry on the modified electrodes. The composite electrodes generated from clays and carbon pastes exhibited a well-defined redox peak of ferri/ferrocyanide and appeared to be more sensitive than bare carbon paste electrodes.

Keywords: Clay, Côte d'Ivoire, modified electrode, Carbon paste electrode

1. Introduction

For centuries, humans have utilized clay to produce tools in a variety of fields. Clay minerals are commonly employed in pharmacy, cosmetics, ceramics, and the manufacturing of bricks for construction purposes. In the field of chemistry, clay's applications are vast and include the development of functional solid catalysts, adsorbents, ion exchangers, and electrochemical sensors, as reported in several studies (Moraes et al., 2017 ; Supelano-García et al., 2020 ; Crapina et al., 2021 ; Maghe et al., 2012).

Clay minerals are natural materials primarily composed of hydrated aluminum silicates, commonly known as phyllosilicates, with a particle size smaller than 2 μm. Phyllosilicates belong to the silicate family (aluminosilicates) and possess a sheet-like structure. Each sheet consists of a stacking of siliceous (T-layer) and aluminous (O-layer) flat layers that are interconnected (Murray, 2006). According to their structure, clays are classified into various classes or groups, such as smectites, montmorillonite, mica (illite), kaolinite, vermiculite, and more (Shichi & Takagi, 2000). The applications of clays depend on their mineral structure, chemical composition, and physicochemical properties.

In recent years, natural alumino-silicate minerals have gained significant attention in the industrial and environmental sectors due to their abundance, cost-effectiveness, and, most importantly, their low environmental impact (Bibi et al., 2016 ; Moussout et al., 2020). These minerals are known as microporous materials widely utilized in chemistry for their high surface area, ion exchange capability, adsorptive capacity, molecular sieving ability, size selectivity, and excellent chemical and thermal stability (Olaremu, 2015 ; Ombaka, 2016). Their versatility has led to an increasing use of clay minerals as modifying agents in the development of modified electrodes (Ebunang et al., 2022 ; Lubna et al., 2022), particularly in the field of novel electrochemical sensors.

However, as regards to carbon paste electrode (CPE) modified with clay, it is a complex heterogeneous system. The use of such electrodes requires a thorough characterization to understand the phenomena of charge and mass transfer in a mixture: solids, liquid, conductors, and insulators. In addition, the origin, composition, and structure of clay included in the paste can impact the electrode response (Mousty et al, 2004; Gómez et al, 2011). Therefore, a well characterization of clay is primordial in the elaboration of clay modified carbon paste electrode.

In Côte d'Ivoire, there are numerous clay sites that have not been thoroughly studied (Konan et al., 2006). Since 1994, several papers have been published focusing on various aspects and characteristics of different clay sites (Sei et al., 2002; Andji et al., 2009; Yoboue et al., 2014; Coulibaly et al., 2014). Recently, Ivorian natural clays have been utilized for various applications based on their physicochemical properties (Coulibaly et al., 2018; Kpangni et al., 2008; Konan et al., 2007). However, to the best of our knowledge, the utilization of Ivorian clay in modified carbon paste electrodes has not been studied.

In this work, new carbon paste electrode modified with natural clay from Côte d'Ivoire was elaborated for the potential detection of organic pollutants. Clay and clay modified electrode were thoroughly characterized using microscopic and electrochemical techniques. The analytical performance of the newly developed sensor was evaluated by studying the electrochemical behavior of the ferri/ferrocyanide couple as redox probes on both the bare and modified electrodes.

2. Method

2.1 Regents and Materials

All chemicals used in the experiment were of analytical grade. Graphite powder with a particle diameter (ø) of 0.1 mm was purchased from Sigma Aldrich. Potassium hexacyanoferrate (II) trihydrate ($K_4[Fe(CN)]_6 \cdot 3H_2O$) was obtained from Scharlau Chemie S.A. Solutions were prepared using distilled water. Potassium perchlorate ($KClO_4$) with a purity of 99.5% from Merck was used as the supporting electrolyte. The firm Dp-pharma paraffin oil was employed. The experiments were conducted at a room temperature of 25°C.

Two types of electrodes were used : a carbon paste electrode and a modified carbon paste electrode, both serving as working electrodes. A saturated silver electrode (Ag/AgCl, KCl_{sat}) was employed as the reference electrode (RE), and a platinum wire was used as the counter electrode (CE).

Clay samples were collected from three different regions in Côte d'Ivoire, which are located in the south and mid-west of the country. The Agban sample (AG) was collected at Bingerville (5.3504° N, 3.8757° W), the Adiaho sample (AD) was collected at Bonoua (5.2712° N, 3.5939° W), and the Zuenoula sample (ZU) was collected at Zuenoula (7.4240° N, 6.0520° W). The samples were collected at a depth of twenty meters for the Adiaho and Zuenoula samples, and fifteen meters for the Agban sample

2.2 Preparation of working electrode

2.2.1 Carbon Paste Electrode

The carbon paste electrode CPE was prepared by mixing 1 g of graphite powder and 300 µL of paraffin oil using mortar and pestle until homogenous paste was obtained. The paste was then incorporated into the electrode cavity and polished on smooth paper. A platinum wire provided the electrical contacts. The electrode surface could be renewed by simple extrusion of a small amount of paste from the tip of the electrode. Before each use of CPE, it was rubbed with a piece of paper until a smooth surface was observed.

2.2.2 Modified Carbon Paste Electrode (MCPE)

2.2.2.1 Clay preparation

Each collected clay sample was carefully dried in the shade for several days to remove any moisture. Once dried, the samples were ground and sieved using a 100 µm sieve to obtain a consistent particle size. In order to perform structural characterization of the clay, the samples underwent a pretreatment process. This involved washing and decantation to obtain a more uniform product for subsequent analytical experiments.

Separation was performed on different clay granulometric particle sizes by sedimentation, decantation, centrifugation, and ultracentrifugation according to Stocke's law. This law expresses the limit speed of sedimentation as a function of the diameter (D) of a solid particle of specific mass γs in a liquid of specific mass and viscosity (Nasri et al, 2016). In principle, sedimentometry is a test that completes the particle size analysis by sieving for fractions below 80µm. Its purpose is the determination of sand, silt, and clay content.

2.2.2.2 Modified Electrode Preparation

The modified carbon paste electrode (MCPE) was prepared using a similar procedure. First, weighed amounts of clay and graphite powder were thoroughly mixed with paraffin oil. Various proportions of clay to graphite powder (w(clay)/w(G)) were used until a uniformly mixed paste was obtained. The resulting paste was then packed tightly into the electrode's cavity through vigorous packing. To maintain the electrode's performance, the surface could be renewed easily by extruding a small amount of paste from the electrode's tip. Additionally, prior to each use, the electrode surface was carefully rubbed with a piece of paper until a smooth surface was achieved.

2.3 Instrumentation

2.3.1 Characterization of Clay

The density of the clay samples was determined using a pycnometer. Various techniques were employed to evaluate the properties of the clays, including physico-chemical composition studies, X-ray diffraction (XRD), Fourier transform infrared spectroscopy (FTIR), and scanning electron microscopy (SEM). These techniques allow comprehensive information about the physico-chemical properties, mineral composition, morphological characteristics, and chemical composition of the clay samples.

X-ray diffraction (XRD) was utilized to analyze the structure and composition of clay minerals. The analysis was performed using CuK_{α} radiation (λ = 1.5406 Å) on a Brüker D8 Advance diffractometer, with a generator current of 40 mA and voltage of 40 kV. Data collection was carried out over a 2θ angular range of 5-60° with a step size of 0.02°s^{-1}.

Scanning electron microscopy (SEM) was employed for morphological characterization of the clay samples. The measurements were conducted using a Hirox SH 4000 model SEM in Europe.

To identify functional groups present in the clay samples, Fourier-transform infrared (FTIR) spectroscopy was performed using a Thermofisher Scientific Nicolet 380 spectrometer. The transmission mode was used, where a mixture of potassium bromide (KBr) pellets and a small quantity of the ground sample (a few mg) was prepared. The acquisitions were made between 4000 and 400 cm^{-1}, using 64 scans with a resolution of 2 cm^{-1}.

Chemical analysis of the clay samples was conducted using X-ray fluorescence (XRF). A Thermo Fisher Scientific Energy Dispersive (EDXRF) apparatus was utilized, with a maximum voltage of 40 kV and a maximum energy of 40 keV.

2.3.2 Characterization of the Electrode

Cyclic voltammetric measurements were performed using a computer-controlled potentiostat (PalmSens, Ecochemie, Netherlands) and PSTrace software. A conventional three electrodes cell (10 mL) consisting of a carbon paste electrode (CPE) as working electrode, a $Ag/AgCl,KCl_{sat}$ as reference electrode and a Pt wire as counter electrode, was used. The solutions pH was measured using a digital pH meter (Hanna Instruments, USA). Each individual experiment was performed at least three times and the results were averages.

3. Results and Discussion

3.1 Characterization of Clays

It is widely recognized that natural clay often contains impurities and exhibits heterogeneity. Table 1 presents the results pertaining to the particle size distribution of the three clay samples under investigation. These findings indicate that the collected samples consist of a mixture of particles with varying sizes. However, it is important to note that clay minerals, as natural materials, typically have particle sizes smaller than 2 µm (Uddin, 2017). Accordingly, the clay content, defined as the fraction below 2 µm, is determined to be approximately 29.66% for sample AD, 57.667% for sample AG, and approximately 18% for sample ZU.

Table 1, which displays the different fractions of the materials, shows that the studied samples comprise a combination of sand, silt, and clay components.

Table 1. Clays sizes

	particle size distribution (µm)		
	> 50µm	**2µm- 50µm**	**< 2µm**
Agban (AG)	37.5	4.83 ±1.33	57.67±1.31
Adiaho (AD)	40	30.33±1.53	29.67±1.53
Zuénoula (ZU)	52	29.67±0.58	18.33±0.58

The results obtained from the pycnometer measurements indicate a range of densities from 2 to 3.6, with values of 2; 2.67; and 3.64 for samples AG, AD, and ZU, respectively. Referring to the work of Deer et al. (1966), the density ranges for various clay minerals are as follows: 2.0–2.6 for Smectites, 2.61–2.68 for Kaolinites, and 2.6–3.3 for Chlorites. The density value obtained for sample AG aligns with the description of Smectites, while samples AD and ZU appear to correspond to Kaolinites and Chlorites, respectively.

However, it is important to note that these results alone do not allow us to conclusively determine the nature of the samples. The observed density values suggest that the samples likely consist of a mixture of different types of clay minerals. To gain a more accurate understanding of the composition, further analysis and characterization techniques are required.

Thus, while the obtained density values are consistent with certain clay mineral structures, additional investigations are needed to precisely identify the nature and composition of the clay minerals in the samples.

The X-ray diffraction (XRD) patterns of the samples are presented in Figure 1AD, Figure 1AG, and Figure 1 ZU. The diffractograms exhibit distinct diffraction peaks at 2θ = 12°, 25°, and 35°, as well as 26°, 36°, and 50°. These peaks correspond to the characteristic crystallographic phases of kaolinite (2θ = 12°, 25°, and 35°) and quartz (2θ = 26°, 36°, and 50°), as reported in the literature (Meite et al., 2020; Sei et al., 2004).

The XRD patterns obtained for all three clay samples (Figure 1) indicate a high content of kaolinite, as evidenced by the presence of its characteristic peaks at 2θ = 12°, 25°, and 35°. This observation suggests that the investigated samples primarily consist of kaolinite. However, the XRD patterns also reveal additional peaks, indicating the presence of other minerals as impurities in the samples. The randomly oriented powder diffractograms unveil the presence of small amounts of feldspar.

The XRD analysis further confirms the presence of iron compounds, silicate phases, quartz minerals (SiO_2), and various clay minerals such as kaolinite ($Si_2Al_2O_5(OH)_4$), illite ($KAl_2(Si_3Al)O_{10}(OH)_2$), and goethite (FeOOH). These identified minerals align with those commonly found in clayey raw materials of Côte d'Ivoire (Meite et al., 2020; Kouadio et al., 2022).

Therefore, the XRD patterns of the clay samples demonstrate a dominant presence of kaolinite, along with the presence of other minerals as impurities. The identified mineral composition is consistent with previous studies on clayey raw materials from Côte d'Ivoire (Meite et al., 2020; Kouadio et al., 2022).

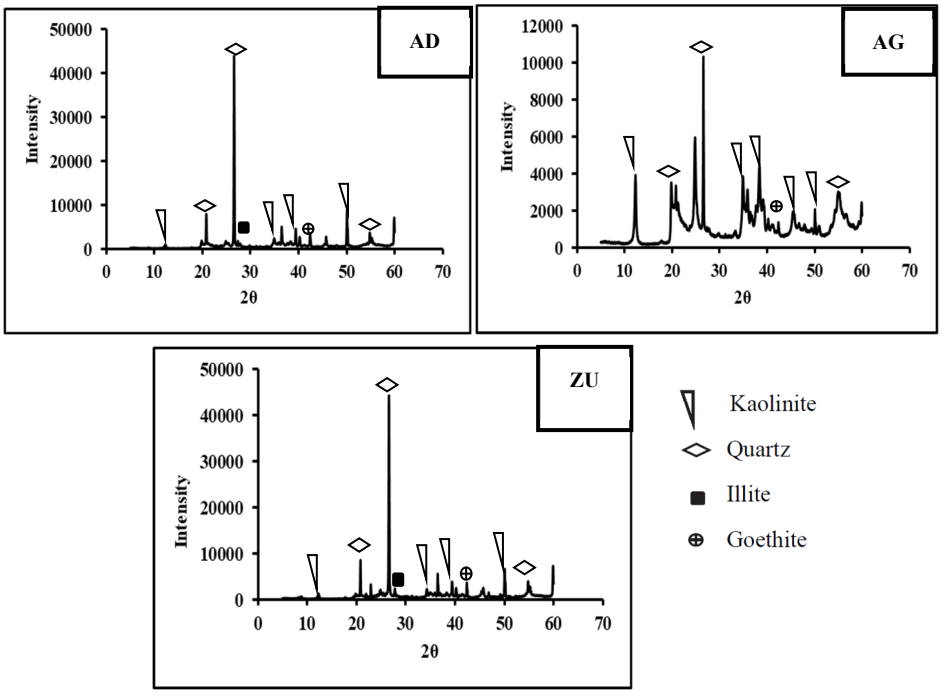

Figure 1. XRD diffractograms of clays: Adiaho (AD); Agban (AG) and Zuenoula (ZU)

Figure 2 displays the SEM images of the clay samples, providing insights into their morphology. The images reveal the presence of large aggregates composed of platelets arranged in a scale-like texture. These randomly oriented platelets are observed in all samples, although the AD sample (Figure 2A) exhibits an interlocking aspect.

Several authors, including Suzuki et al. and Caillère et al. (Zuzuki et al., 2013; Caillère et al., 1982), have described kaolinite particles at the nanoscale as having a laminar structure of pseudo-hexagonal platelets. The morphology depicted in Figure 2 aligns with the typical appearance of kaolin, characterized by heterogeneous layered sheets of varying sizes. Additionally, a significant quantity of quartz mineral, which serves as an impurity in kaolin, is observed.

These findings are consistent with previous studies conducted on clay samples from Côte d'Ivoire by various authors (Konan et al., 2007; Meite et al., 2020; Kouadio et al., 2022; Konan et al., 2010). These studies consistently reported that the clay samples predominantly consist of kaolinite. Therefore, the SEM results support the XRD findings and confirm the prevalence of kaolinite as the primary mineral phase present in all the studied clays.

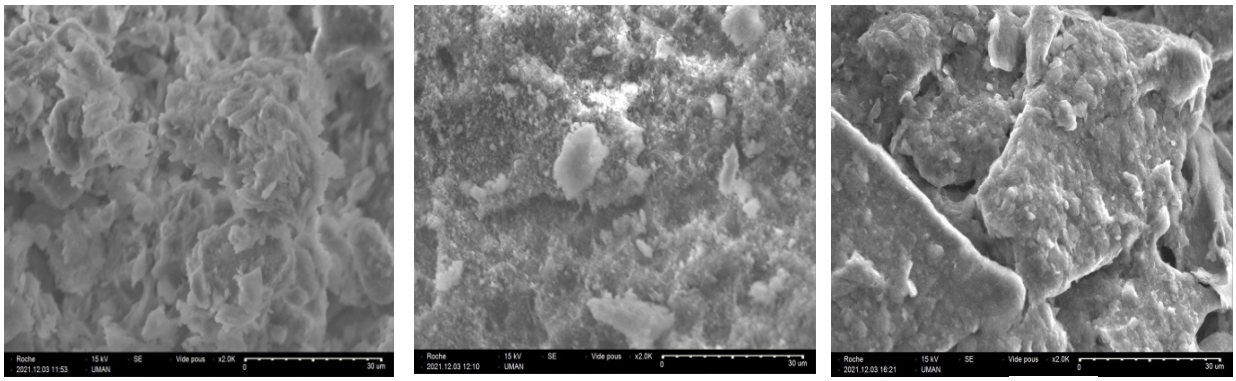

(A) (B) (C)

Figure 2. SEM images of clays :(A) Adiaho (AD); (B) Agban (AG) and (C)Zuenoula (ZU)

The elemental analysis conducted with Energy Dispersive X-ray Spectroscopy (EDS) provides valuable information about the chemical composition of the clay samples and highlights the variations between the three samples. Figure 3 presents the percentage composition of various components, including Si, Al, Ti, Fe, K, Mg, Na, O, Ca, and C. These results indicate the relative abundance of these elements in the clay samples. The presence of silicon (Si) and aluminum (Al) is expected, as they are major constituents of clay minerals. The percentage of Si and Al can provide insights into the type and composition of clay minerals present in the samples.

Other elements such as titanium (Ti), iron (Fe), potassium (K), magnesium (Mg), sodium (Na), oxygen (O), calcium (Ca), and carbon (C) may also be detected in varying amounts, depending on the specific characteristics of the clay samples and their sources. The presence and quantities of these elements contribute to understanding the overall chemical composition and potential impurities in the clay samples.

The differences observed in the percentage composition of the elements among the three clay samples suggest variations in their chemical makeup. These differences may be attributed to variations in the mineralogical composition, geological origin, and processing of the clay samples.

This analysis of the clay minerals reveals some noteworthy differences between the samples. In the case of ZU, the presence of calcium (Ca) is detected, while it is not detected in the AD and AG clay minerals. This indicates a variation in the elemental composition of the three samples.

Furthermore, the analysis shows that the Al/Si atomic concentration ratio is close to 1.0 for AG, which aligns with the expected chemical composition of kaolinite ($Al_2Si_2O_5(OH)_4$). This suggests that the AG sample predominantly consists of kaolinite. On the other hand, AD and ZU exhibit a higher silicon (Si) content compared to aluminum (Al). This higher Si content may be attributed to the presence of a significant concentration of quartz in these clay minerals. Quartz is known for its high Si content and is commonly found as an impurity in clay samples.

Additionally, the analysis reveals the presence of several components in small quantities and varying proportions, including titanium (Ti), potassium (K), magnesium (Mg), sodium (Na), and calcium (Ca). These elements may be present as minor constituents or impurities in the clay samples.

These results provide valuable insights into the elemental composition and differences observed among the AD, AG, and ZU clay samples.

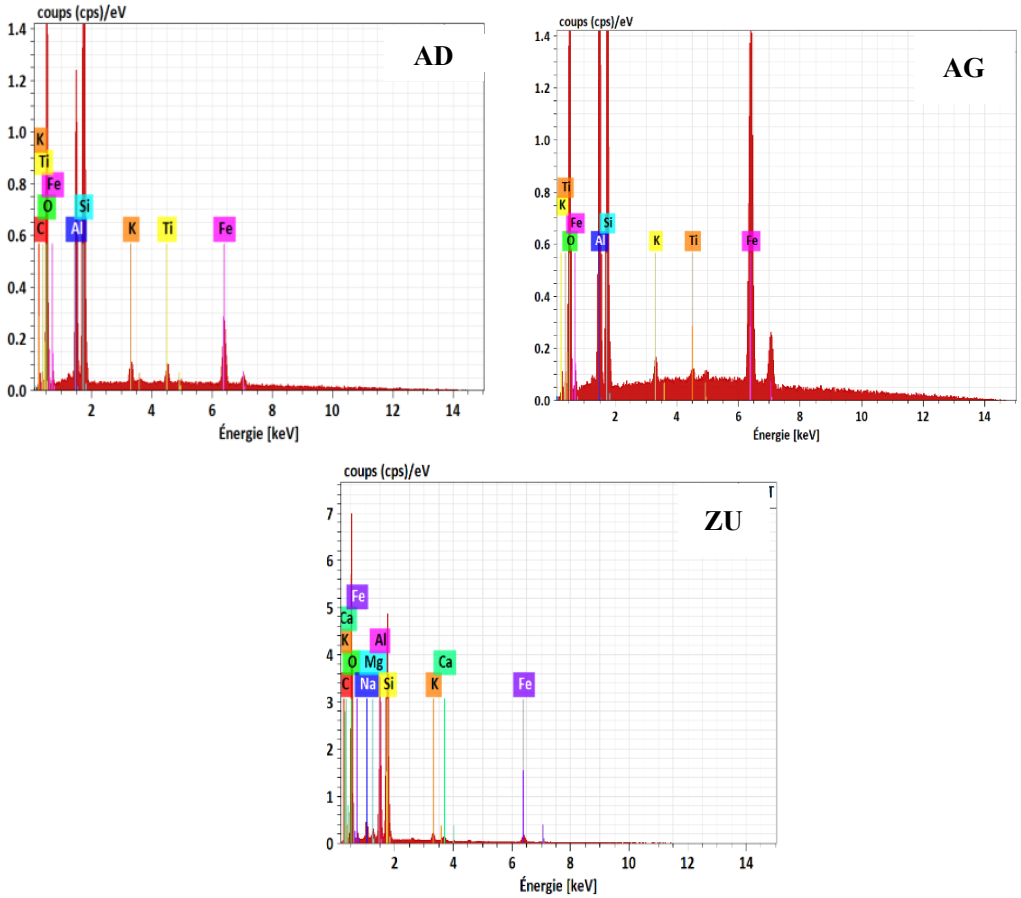

Figure 3. EDS spectrum of clays elemental analysis of Adiaho (AD); Agban (AG) and Zuenoula

The FTIR (Fourier Transformed Infrared) spectroscopy analysis was conducted to complement the X-ray diffraction results and assess the surface functional groups present in the AD, AG, and ZU clay samples. The FTIR spectra (Figure 4) exhibit similar vibration bands across all samples, consistent with observations of clay materials.

The spectra reveal prominent bands at around 3620 cm^{-1} and 3700 cm^{-1} in all samples. These bands are associated with the stretching vibrations of hydroxyl (OH) groups. According to Quantin (1993), the band at 3700 cm^{-1} represents the external OH group, while the band at 3620 cm^{-1} corresponds to the internal OH group in kaolinite.

Furthermore, a weaker band at 1634 cm^{-1} is observed, which can be attributed to the stretching vibration of the Al–OH bond. A symmetrical Si-O-Si stretching vibration band at 1032 cm^{-1} is evident in all spectra, indicative of the characteristic vibrations of kaolinite and illite (Kouakou et al, 2022). Other distinctive kaolinite bands are observed at 1006 cm^{-1}, 938 cm^{-1}, and 536 cm^{-1}. It is worth noting that absorption bands in the OH stretching region of sheet silicates can overlap in the range of 3700-3500 cm^{-1} (Eba et al, 2011).

The absorption bands at 797 cm^{-1} and 779 cm^{-1} can be associated with quartz (Koshchug et al, 2020). Moreover, the average intensity bands observed at 696 cm^{-1}, 755 cm-1, and 796 cm^{-1} in the IR spectrum correspond to the stretching vibrations of the Si-O-Al bonds and the OH hydroxyls perpendicular to the surface, also known as translational OH (Atsé et al, 2022; Aké et al, 2022).

These findings confirm the presence of characteristic functional groups in the clay samples and align with previous studies conducted on clay materials in the region (Atsé et al, 2022; Aké et al, 2022). The FTIR analysis provides valuable information about the molecular vibrations and surface functional groups, further supporting the identification of the clay mineral phases present in the AD, AG, and ZU samples.

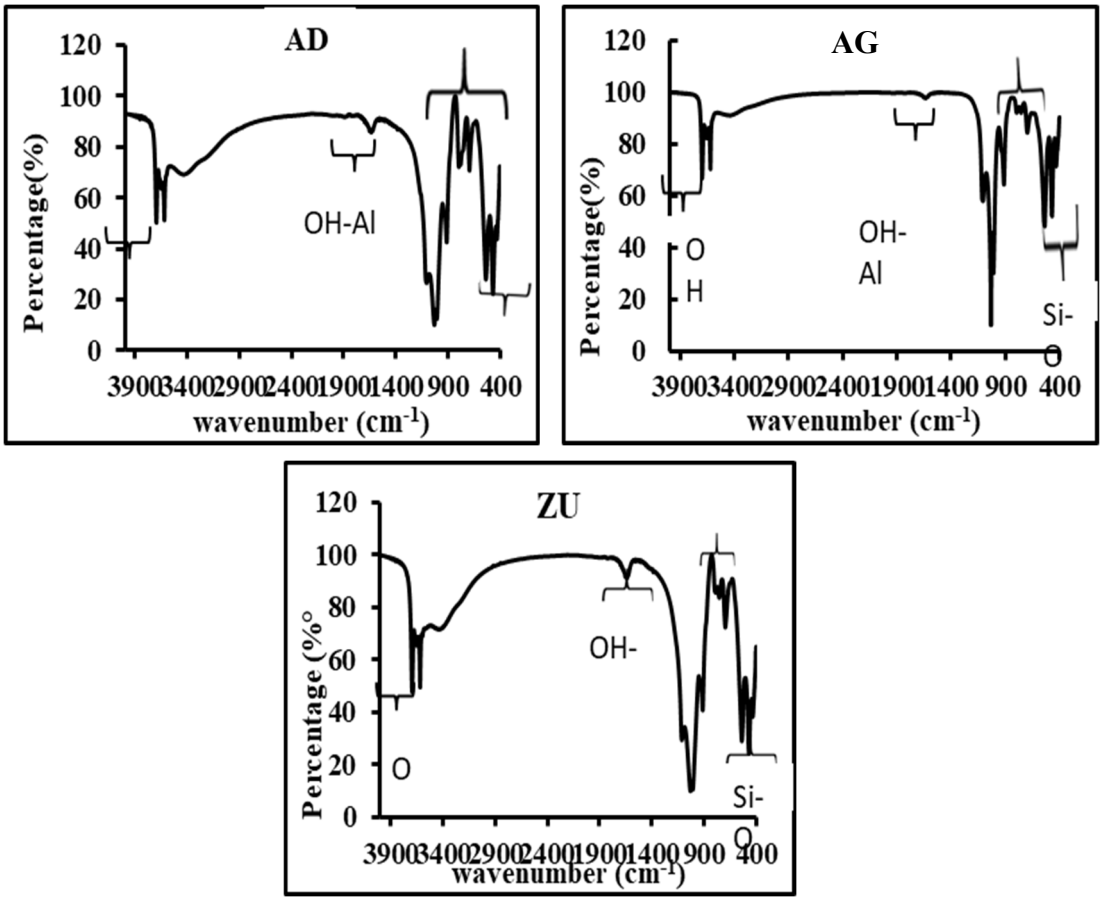

Figure 4. FTIR spectrum of clays: Adiaho (AD); Agban(AG) and Zuenoula (ZU)

The elemental composition of the three clay samples was analyzed, and the oxide content is presented in Table 2. The results confirm that the samples are predominantly composed of aluminum oxide (Al_2O_3) and silicon oxide (SiO_2), indicating their classification as aluminosilicates (Nirmala & Viruthagiri, 2015). The SiO_2/Al_2O_3 ratios for AG, ZU, and AD are 1.72 ; 3.34 ; and 3.87, respectively. These ratios are higher compared to the typical ratio of 1.18 found in kaolinites (Lecomte-Nana et al., 2013). The elevated SiO_2/Al_2O_3 ratios suggest the possible presence of free quartz in a significant proportion within the clay fraction (Gourouza et al., 2013). The excess silica observed can be attributed to the presence of quartz and/or compounds such as 2/1 clay minerals like illite and muscovite (Coulibaly et al., 2020).

Additionally, the clay samples exhibit a relatively large quantity of iron oxide, indicating the presence of ferric phases. The presence of other oxides such as CaO, MgO, Na_2O, K_2O, and TiO_2 is also observed, albeit in low percentages.

These findings further support the aluminosilicate nature of the clay samples, highlighting the elevated SiO_2/Al_2O_3 ratios, the potential presence of free quartz, and the occurrence of ferric phases. The detailed oxide composition presented in Table 2 provides a comprehensive overview of the elemental composition of the clay samples.

Table 2. Chemical composition (mass % oxide) of clays samples

	SiO_2	Al_2O_3	Fe_2O_3	CaO	K_2O	MgO	Na_2O	TiO_2	SiO_2 / Al_2O_3
ZU	64.9	19.4	5.72	0.29	2.26	2.55	0.14	0.78	3.34
AD	68.50	17.67	6.27	0.09	1.23	1.2	0.58	1.31	3.87
AG	50.80	29.48	6.06	0.01	1.01	2.46	-	0.98	1.72

The semi-quantitative mineralogical composition of the three clay samples was determined by summing the values obtained from the qualitative mineralogical analysis. This allows for the calculation of the total chemical composition, as shown in Table 3. The calculation is based on the relationship developed by Njopwouo (). T(a) = Σ Mi x Pi (a), as referenced in Kouadio et al. (2022), where T(a) represents the content (mass %) of oxide a in the clay, Mi represents the content of mineral i (%) in the clay, and Pi(a) represents the proportion of oxide a in mineral.

By applying this relationship, the semi-quantitative mineralogical composition of the three samples was determined, providing valuable insights into their overall chemical composition. These results are found to be consistent with the findings published in the literature by Meite et al. (2020) and Kouakou et al. (2022), further validating the accuracy and reliability of the analysis conducted in this study.

Table 3. Semi-quantitative mineralogical compositions of clays

Echantillons	Quartz	Kaolinite	Illite	Goethite	Total
AD	42.15	30.46	19.57	6.98	99.16
AG	47.71	34.57	10.65	6.74	99.67
ZU	16.11	66.25	8.75	6.37	97.48

3.2 Electrochemical Characterization of Clay Modified Electrode

The ferri/ferrocyanide couple is an ideal electrochemical probe which is widely used on different electrodes for the study of surfaces (Promph et al, 2015; Vogt et al, 2016). In order, to compare the electrochemical properties of bare carbon paste electrode, clay paste electrode and clay modified carbon paste electrode, the redox couple ferricyanide/ferrocyanide was chosen.

Preliminary studies were performed on clay paste electrodes (ClPE) in potassium hexacyanoferrate solution at pH 7. Figure 5 shows a typical Cyclic voltammetry (CV) recorded at a ClPE electrode between –0.4 V and 0.6V.

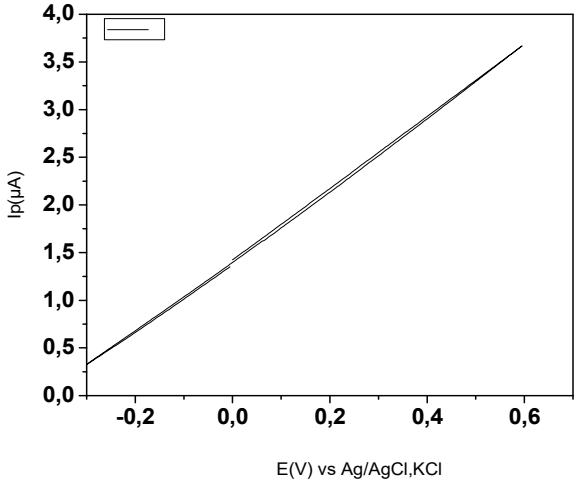

Figure 5. Typical cyclic voltammogram of clay paste electrodes in 1.0 mM [Fe (CN)6] $^{3-/4-}$; pH = 7 at 20 mV s^{-1}

The absence of redox peaks observed on the clay paste electrodes (ClPE) in the cyclic voltammetry (CV) analysis indicates that the ferri/ferrocyanide redox couple is inactive on the ClPE. This suggests either a lack of reduction of Fe $(CN)^{3-}$ or the absence of subsequent re-oxidation of $Fe(CN)^{4-}$ on the ClPE surface. It is possible that the ClPE electrode itself is inactive in this electrochemical system.

The conductivity of clays has been reported to depend on various factors, such as heating temperature, clay pore structure, and soil mineralogy. These factors can influence the electrochemical behavior and conductivity of the clay paste electrodes. Studies conducted by El Kasmi et al. (2016), Ranđelovićе et al. (2017), and Xu et al. (2019)

have highlighted the relationship between clay conductivity and these factors. Therefore, the lack of activity observed on the ClPE electrodes could be attributed to their specific conductivity properties influenced by these factors.

The electrochemical behavior of clay-modified electrodes was tested by cyclic voltammetry (CV) in potassium hexacyanoferrate solution. Figure 6 represents the responses obtained between 0.0 V and +0.7 V (vs. AgCl/Ag) on CPE, and CPE modified by 5% of clay AD (ADCPE), 5% of clay AG (AGCPE) and 5% of clay ZU (ZUCPE) respectively in a solution containing 1 mM $[Fe(CN)_6]^{3/4}$ (1:1) at 20 mV/s.

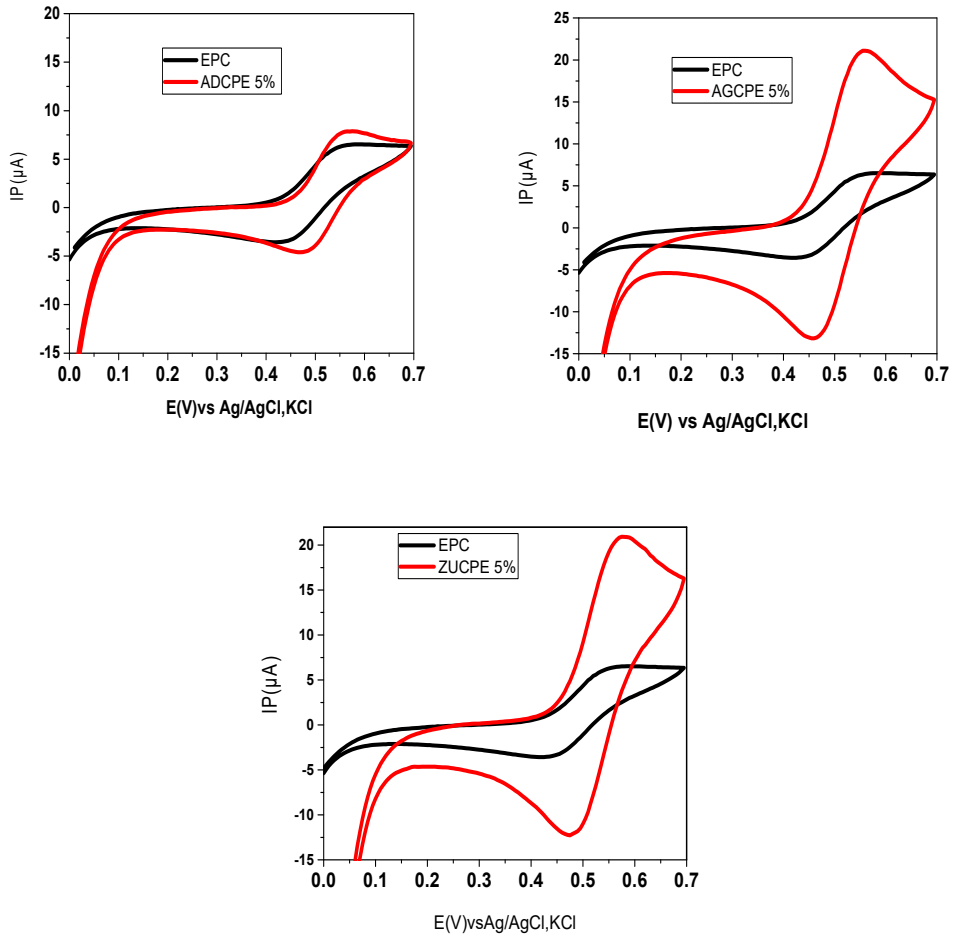

Figure 6. Cyclic voltammograms of bare and modified electrodes in 1.0 mM [Fe (CN)6]3-/4- at 20 mV s-1and pH=7; MCPE (red) and CPE (black)

The system ferri/ferrocyanide showed a different behavior on CPE and MCPEs. The oxidation and reduction peak currents observed increase for the modified CPEs versus unmodified electrode (see Table 4). A slight decrease in (Epa) was observed for ADCPE while it increases for AGCPE and ZUCPE. The value of ratio between the anodic and cathodic peak currents (Ipa/Ipc) is superior to 1; this shows a quasi-reversible of the system because the ideal reversible process is characterized by the ratio Ipa/Ipc approaches unity. Intensity of peaks on CPE system was markedly lower than those on MCPE, which can indicative of hindered diffusion on CPE and the improvement of the electron transfer rate on MCPE. Another characteristic parameter is the separation of the peak potentials ΔEp. The theoretical value for ΔEp in reversible process is 60 mV, and it is independent of scan rate. Here, with a difference of 100 mV, ΔEp characterizes a slow electron transfer kinetics due to several factors, such as uncompensated solution resistance and non-linear diffusion (Xiao et al., 2014; Aristov & Habekost, 2015).

Table 4. Reduction/oxydation potentials. reduction/oxydation peaks. peaks separation and ratio of the anodic and cathodic current for1.0 mM $[Fe(CN)_6]^{3-/4-}$ at 20 mV s^{-1} and pH=7 on CPE. ADCPE. AGCPE and ZUCPE

	Ep_c (V)	Ep_a (V)	ΔEp(V)	Ip_a(μA)	$\lvert Ip_c(\mu A)\rvert$	$\lvert Ip_a/Ip_c\rvert$
CPE	0.44	0.54	0.10	6.10	4.00	1.53
ADCPE 5%	0.385	0.56	0.10	7.46	3.85	1.93
AGCPE 5%	0.45	0.56	0.10	21.03	13.22	1.59
ZUCPE 5%	0.48	0.57	0 .11	21.50	12.44	1.73

The electrochemical behavior of clay-modified electrodes, namely ADCPE, AGCPE, and ZUCPE, was investigated by altering the clay content in the carbon paste. It has been reported in previous studies (Lubna et al., 2022; Salih et al., 2017; Eslami et al., 2014) that the clay content in carbon paste can significantly influence the voltammetric responses and sensor properties. In this study, the proportion of clay in the carbon paste was varied from 3% to 20% to assess its impact on the electrochemical performance.

Figure 7 illustrates the responses of the redox probe as a function of the clay percentage in the carbon paste. By systematically altering the clay content, the aim was to understand the relationship between clay concentration and the resulting electrochemical behavior.

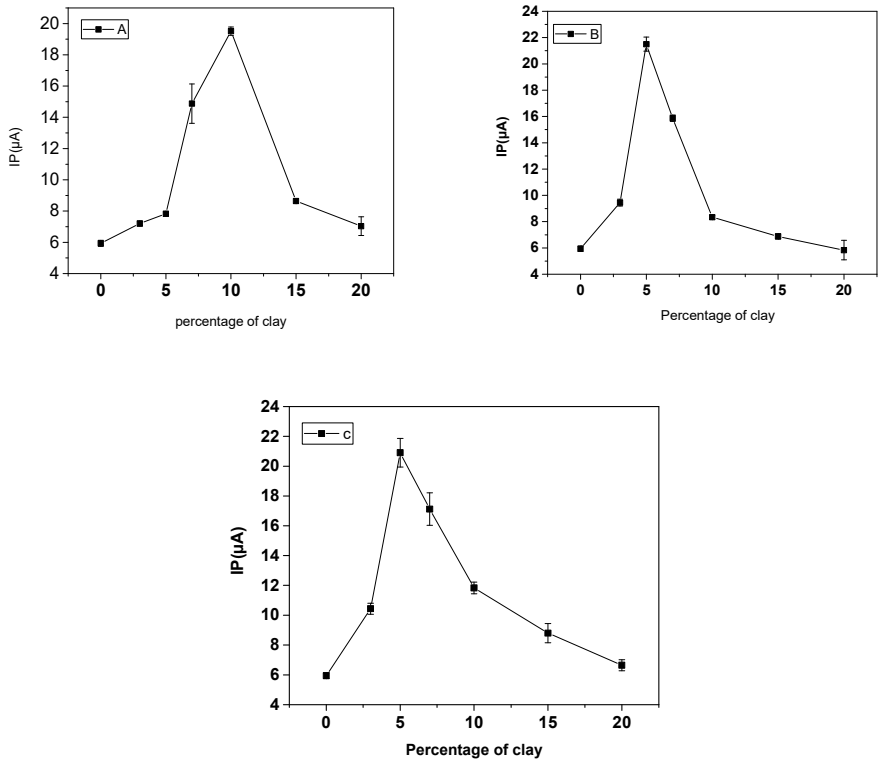

Figure 7. The plot of peak current versus clay amounts in paste carbone: (A) Adiaho (AD) (B)Agban (AG) and (C) Zuenoula (ZU)

The behavior of the ferri/ferrocyanide redox couple varied with the concentration of clay in the carbon paste. The highest anodic current peaks were obtained when the clay content was 5% for AG and ZU, and 10% for AD. However, beyond these concentrations, a significant decrease in current peaks was observed. This decrease can be attributed to a reduction in the carbon content of the electrode material. As shown in Figure 5, the clays used in

this study appear to be non-conductive materials. It has been reported that a high clay content can lead to the saturation of the electrode surface and consequently reduce the oxidation current of the reactant (Salih et al., 2017).

Nevertheless, the properties of these clays can be modified to enhance the sensitivity of the sensors. In order to avoid potential saturation of the electrode, it was determined that a clay concentration of 5% for AG and ZU, and 10% for AD would be suitable for future studies. These concentrations strike a balance between maximizing the anodic current peaks and maintaining the electrode's performance

4. Conclusion

This study investigated the potential of composite materials based on clay and carbon paste for the development of electrochemical sensors. The three clays obtained from Côte d'Ivoire (Adiaho, Agban, & Zuenoula) were thoroughly characterized using X-ray diffraction (XRD), scanning electron microscopy (SEM), EDS-mapping analysis, and Fourier transform infrared spectroscopy (FTIR). The characterization results consistently identified kaolinite as the dominant component in all three clay samples.

The electrochemical behavior of the ferri/ferrocyanide redox couple was then evaluated on clay-modified carbon paste electrodes using cyclic voltammetry. The results demonstrated that the modification of the electrodes with varying amounts of clay in the carbon paste had a significant impact on the response of the analyte.

Based on these findings, it can be inferred that the modified electrodes utilizing Ivorian clays, hold potential for future electroanalytical investigations. These clay-based composite materials offer new opportunities for the development of sensitive and reliable electrochemical sensors. Further research and optimization of the clay content in the carbon paste are warranted to fully harness the capabilities of these modified electrodes and explore their application in various electroanalytical techniques.

Conflicts of Interest

The authors declare no conflicts of interest regarding the publication of this paper.

References

Ake, P. A., COULIBALY, V., KEDI, A. B., Joseph, S. E. I., & OYETOLA, S. (2022). Study of the status of iron in clay materials from Côte d'Ivoire for their use as phosphate adsorbents. *Sciences des Structures et de la matière*, *6*(1).

Andji, J. Y. Y., Toure, A. A., Kra, G., Jumas, J. C., Yvon, J., & Blanchart, P. (2009). Iron role on mechanical properties of ceramics with clays from Ivory Coast. *Ceramics International*, *35*(2), 571-577. https://doi.org/10.1016/j.ceramint.2008.01.007

Aristov, N., & Habekost, A. (2015). Electrochromism of methylviologen (paraquat). *World J. Chem. Educ*, *3*(4), 82-86. https://doi.org/10.12691/wjce-3-4-1

Atsé, W. A., Essi, M. M. M. M., Doubi, B. I. H. G., Kamagaté, M., Aké, A. P., & Kouamé, A. N. (2022). Physico-Chemical Characterization of Two Dabou Clays with a View to Use Them in the Treatment of Dyeing Wastewater. *Journal of Minerals and Materials Characterization and Engineering*, *10*(6), 505-517. https://doi.org/10.4236/jmmce.2022.106036

Bibi, I., Icenhower, J., Niazi, N. K., Naz, T., Shahid, M., & Bashir, S. (2016). Chapter 21-Clay Minerals: Structure, Chemistry, and Significance in Contaminated Environments and Geological CO2 Sequestration. In M. N. V. Prasad, & K. Shih (Eds.), *Environmental Materials and Waste: Resource Recovery and Pollution Prevention* (pp. 543-567). New York: Elsevier Inc. https://doi.org/10.1016/B978-0-12-803837-6.00021-4

Caillere, S., Henin, S., & Rautureau, M. (1982). *Mineralogie des Argiles*（2th Ed.). Masson, Paris

Cipriano Crapina, L., Dzene, L., Brendlé, J., Fourcade, F., Amrane, A., & Limousy, L. (2021). Clay-Modified Electrodes in Heterogeneous Electro-Fenton Process for Degradation of Organic Compounds: The Potential of Structural Fe (III) as Catalytic Sites. *Materials*, *14*(24), 7742. https:// doi.org/10.3390/ma14247742

Coulibaly, B., Guillaume Pohan, L. A., Kambiré, O., Kouakou, L. P. S., Goure-Doubi, H., Diabaté, D., & Ouattara, L. (2020). Valorization of green clay from Bouaflé (Ivory Coast) in the simultaneous elimination of organic pollutants and metallic trace elements by adsorption: Case of methylene blue and cadmium ions. *Chemical Science International Journal*, *29*(8), 37-51. https://doi.org/10.9734/CSJI/2020/v29i830200

Coulibaly, V., Kédi, A. B., Sei, J., & Oyetola, S. (2018). Reactivity of Clays Consummated in Côte d'Ivoire in Digestive Conditions: Bioavailability of Mineral Elements. *Asian Journal of Applied Sciences*, *6*(5). https://doi.org/10.24203/ajas.v6i5.5362

Coulibaly, V., Sei, J., Koffi, L. K., Oyetola, S., Jdid, E.-A. & Thomas, F. (2014). Mineralogical and Chemical Characteristics of Clays Consumed in the District of Abidjan (Côte D'Ivoire). *Materials Sciences and Applications, 5*, 1048-1059. https://doi.org/10.4236/msa.2014.514108

Deer, D. A., Howie, R. A., & Zussman, J. (1966). *An Introduction to the Rock Forming Minerals*. Longman Scientific & Technical, Essex, England.

Eba, F., Nkoumbou, C., Ondo, J. A., Omva-Zué, J., Yvon, J., & Njopwouo, D. (2011). Mineralogical and physico-chemical characterization of clay from Bikougou (Gabon). *Annales de la Faculté des Sciences, Université de Yaoundé*, *1*, 45-56.

Ebunang, D. V. T., Tajeu, K. Y., Pecheu, C. N., Jiokeng, S. L. Z., Tamo, A. K., Doench, I., ... & Ngameni, E. (2022). Amino-Functionalized Laponite Clay Material as a Sensor Modifier for the Electrochemical Detection of Quercetin. *Sensors*, *22*(16), 6173. https://doi.org/10.3390/s22166173

El Kasmi, S., Lahrich, S., Farahi, A., Zriouil, M., Ahmamou, M., Bakasse, M., & El Mhammedi, M. A. (2016). Electrochemical determination of paraquat in potato, lemon, orange and natural water samples using sensitive-rich clay carbon electrode. *Journal of the Taiwan Institute of Chemical Engineers*, *58*, 165-172. https://doi.org/10.1016/j.jtice.2015.06.039

Eslami, E., Farjami, F., Aberoomand Azar, P., & Saber Tehrani, M. (2014). Adsorptive stripping voltammetric determination of imipramine and amitriptiline at a nanoclay composite carbon ionic liquid electrode. *Electroanalysis*, *26*(2), 424-431. https://doi.org/10.1002/elan.201300557

García, I. S., Gómez, C. A. P., Gómez, J. A. M., & Vargas, C. A. P. (2020). Caracterización físico-química de mezclas de arcilla mineral de Boyacá-Colombia/Physico-chemical characterization of clay mineral mixtures from Boyacá-Colombia. *Dyna*, (213), 116. https://doi.org/10.15446/dyna.v87n213.84592

Gómez, Y., Fernández, L., Borrás, C., Mostany, J., & Scharifker, B. (2011). Characterization of a carbon paste electrode modified with tripolyphosphate-modified kaolinite clay for the detection of lead. *Talanta*, *85*(3), 1357-1363. https://doi.org/10.1016/j.talanta.2011.06.014

Gourouza, M., Zanguina, A., Natatou, I., & Boos, A. (2013). Caracterisation d'une argile mixte du niger *Rev. CAMES - Sciences Struct. Mat., 1*, 29-39

Jaber, L., Elgamouz, A., & Kawde, A. N. (2022). An insight to the filtration mechanism of Pb (II) at the surface of a clay ceramic membrane through its preconcentration at the surface of a graphite/clay composite working electrode. *Arabian Journal of Chemistry*, *15*(12), 104303.

Konan, K. L., Sei, J., Soro, N. S., Oyetola, S., Gaillard, J. M., & Bonnet, J. P. (2006). Caractérisation de matériaux argileux du site d'Azaguie-Blida (Anyama, Côte D'Ivoire) et détermination des propriétés mécaniques de produits céramiques. *Journal de la Société ouest-africaine de chimie*, (21), 35-43.

Konan, K. L., Soro, J. Y., Andji, S., Oyetola, S., & Kra, G. (2010). Comparative Study of Dihydroxylation/Amorphization in Two Kaolins with Different Crystallinity. *Journal de la Société Ouest-Africaine de Chimie*, *30*, 29-39.

Konan, K.L, Peyratout, C., Bonnet, J.-P., Smith,A., Jacquet A., Magnoux, P. & Ayrault, P.(2007). Propriétés de surface des suspensions de kaolin et d'illite en milieu hydroxyde de calcium concentré. *Journal of Colloid and Interface Science, 307*(1), 101-108. https://doi.org/10.1016/j.jcis.2006.10.085

Koshchug, D. G., Koshlyakova, A. N., Balitsky, V. S., & Vyatkin, S. V. (2020). Infrared and Raman spectroscopy study of Si1− xGexO2 solid solutions with α-quartz structures. *Spectrochimica Acta Part A: Molecular and Biomolecular Spectroscopy*, *233*, 118168. https://doi.org/10.1016/j.saa.2020.118168

Kouakou, L., Kouamé, A., Doubi, B., Méité, N., Kangah, J., Zokou, E., Konan, L. & Andji Y., Y. (2022). Caractérisation de deux matières premières argileuses de Côte d'Ivoire en vue de les valoriser en éco-construction. *Journal de caractérisation et d'ingénierie des minéraux, 10*, 198-208.

Koudia, L. M., Lebouachera, S. E. I., Blanc, S., Joseph, S., Miqueu, C., Pannier, F., & Martinez, H. (2022). Characterization of Clay Materials from Ivory Coast for Their Use as Adsorbents for Wastewater Treatment. *Journal of Minerals and Materials Characterization and Engineering*, *10*, 319-337. https://doi.org/10.4236/jmmce.2022.104023

Kpangni, E. B., Andji, Y. Y. J., Adouby, K., Oyetola, S., Kra, G., & Yvon, J. (2008). Mineralogy of Clay Raw Materials from Cote d'ivoire: Case of the Deposit from Katiola. *Journal of Applied Sciences*, *8*(5), 871-875. https://doi.org/10.3923/jas.2008.871.875

Lecomte-Nana, G., Bonnet, J. P., & Soro, N. (2013). Influence of iron onto the structural reorganization process during the sintering of kaolins. *Journal of the European Ceramic Society*, *33*(4), 661-668. https://doi.org/10.1016/j.jeurceramsoc.2012.10.024

Maghear, A., Cernat, A., Cristea, C., Marian, A., Marian, I. O., & Săndulescu, R. (2012, June). New electrochemical sensors based on clay and carbon micro and nanoparticles for pharmaceutical and environmental analysis. In *Technical Proceedings of the 2012 NSTI Nanotechnology Conference and Expo* (Vol. 1, pp. 574-577). NSTI-Nanotech Santa Clara, CA.

Méité, N., Konan, L. K., Tognonvi, M. T., Doubi, B. I. H. G., Gomina, M., & Oyetola, S. (2021). Properties of hydric and biodegradability of cassava starch-based bioplastics reinforced with thermally modified kaolin. *Carbohydrate Polymers*, *254*, 117322. https://doi.org/10.1016/j.carbpol.2020.117322

Moraes, J. D. D., Bertolino, S. R. A., Cuffini, S. L., Ducart, D. F., Bretzke, P. E., & Leonardi, G. R. (2017). Clay minerals: Properties and applications to dermocosmetic products and perspectives of natural raw materials for therapeutic purposes—A review. *International Journal of Pharmaceutics*, *534*(1-2), 213-219. https://doi.org/10.1016/j.ijpharm.2017.10.031

Moussout, H., Ahlafi, H., Aazza, M., Chfaira, R., & Mounir, C.(2020). Interfacial electrochemical properties of natural Moroccan Ghassoul (stevensite) clay in aqueous suspension. *Helyon, 6*(3), 3634. https://doi.org/10.1016/j.heliyon.2020.e03634

Mousty, C. (2004). Sensors and biosensors based on clay-modified electrodes-new trends. *Appl. Clay Sci, 27*, 159-177. https://doi.org/10.1016/j.clay.2004.06.005

Murray, H. H. (2006). *Applied clay mineralogy: occurrences, processing and applications of kaolins, bentonites, palygorskitesepiolite, and common clays*. Elsevier. https://doi.org/10.1016/S1572-4352(06)02008-3

Nasri, H., Elhammouti, K., Azdimous, A., Achalhi, M. & Bengamra, S. (2016). Caractérisation calcimétrique et Nasri, H., Elhammouti, K., Azdimousa, A., Achalhi, M., & Bengamra, S. (2016). Caractérisation calcimétrique et sédimentométrique des dépôts argileux du bassin néogène de Boudinar (Rif nord-oriental, Maroc): Implication sur l'évolution eustatique et hydrodynamique du bassin et intérêt économique. *J Mater Environ Sci*, *7*, 859-870.

Nirmala, G., & Viruthagiri, G. (2015). A view of microstructure with technological behavior of waste incorporated ceramic bricks. *Spectrochimica Acta Part A: Molecular and Biomolecular Spectroscopy*, *135*, 76-80. https://doi.org/10.1016/j.saa.2014.06.150

Olaremu, A. G. (2015). Physico-chemical characterization of Akoko mined kaolin clay. *Journal of Minerals and Materials characterization and Engineering*, *3*(05), 353. https://doi.org/10.4236/jmmce.2015.35038

Ombaka, O. (2016). Characterization and classification of clay minerals for potential applications in Rugi Ward, Kenya. *African Journal of environmental science and Technology*, *10*(11), 415-431. https://doi.org/10.5897/AJEST2016.2184

Promphet, N., Rattanarat, P., Rangkupan, R., Chailapakul, O., & Rodthongkum, N. (2015). An electrochemical sensor based on graphene/polyaniline/polystyrene nanoporous fibers modified electrode for simultaneous determination of lead and cadmium. *Sensors and Actuators B: Chemical*, *207*, 526-534. https://doi.org/10.1016/j.snb.2014.10.126

Quantin, P. (1993). Spectroscopie infrarouge et Analyse minéralogique quantitative des roches in Spectroscopie infrarouge et analyse minéralogique quantitative des roches: méthode et résultats nouveaux, Bondy: ORSTOM, 39-47.

Ranđelović, M. S., Momčilović, M. Z., Nikolić, G., & Đordević, J. S. (2017). Electrocatalitic behaviour of serpentinite modified carbon paste electrode. *Journal of Electroanalytical Chemistry*, *801*, 338-344. https://doi.org/10.1016/j.jelechem.2017.08.011

Salih, F. E., Achiou, B., Ouammou, M., Bennazha, J., Ouarzane, A., Younssi, S. A., & El Rhazi, M. (2017). Electrochemical sensor based on low silica X zeolite modified carbon paste for carbaryl determination. *Journal of advanced research*, *8*(6), 669-676. https://doi.org/10.1016/j.jare.2017.08.002

Sei, J., Jumas, J. C., Olivier-Fourcade, J., Quiquampoix, H., & Staunton, S. (2002). Role of iron oxides in the phosphate adsorption properties of kaolinites from the Ivory Coast. *Clays and Clay minerals*, *50*(2), 217-222. https://doi.org/10.1346/000986002760832810

Sei, J., Touré, A. A., Olivier-Fourcade, J., Quiquampoix, H., Staunton, S., Jumas, J. C., & Womes, M. (2004). Characterisation of kaolinitic clays from the Ivory Coast (West Africa). *Applied Clay Science*, *27*(3-4), 235-239. https://doi.org/10.1016/j.clay.2004.06.004

Shichi, T. & Takagi, K. (2000). Clay Minerals as Photochemical Reaction Fields. *J. Photochem. Photobiol. C: Photochem. Rev., 1*(2), 113-130. https://doi.org/10.1016/S1389-5567(00)00008-3

Suzuki, T., Nakamura, A., Niinae, M., Nakata, H., Fujii, H., & Tasaka, Y. (2013). Lead immobilization in artificially contaminated kaolinite using magnesium oxide-based materials: Immobilization mechanisms and long-term evaluation. *Chemical engineering journal*, *232*, 380-387. https://doi.org/10.1016/j.cej.2013.07.121

Uddin, M. K. (2017). A review on the adsorption of heavy metals by clay minerals, with special focus on the past decade. *Chemical Engineering Journal*, *308*, 438-462. https://doi.org/10.1016/j.cej.2016.09.029

Vogt, S., Su, Q., Gutiérrez-Sánchez, C., & Nöll, G. (2016). Critical view on electrochemical impedance spectroscopy using the ferri/ferrocyanide redox couple at gold electrodes. *Analytical chemistry*, *88*(8), 4383-4390. https://doi.org/10.1021/acs.analchem.5b04814

Xiao, F., Gu, M., Liang, Y., Dong, M., Zhao, Z., & Zhi, D. (2014). Synthesis, characterization and electrochemical behavior of ferrocene-containing highly branched polyurethane and its application in biosensing. *Journal of Organometallic Chemistry*, *772*, 122-130. https://doi.org/10.1016/j.jorganchem.2014.08.016

Xu, Y., Zeng, Z., & Lv, H. (2019). Effect of temperature on thermal conductivity of lateritic clays over a wide temperature range. *International Journal of Heat and Mass Transfer*, *138*, 562-570. https://doi.org/10.1016/j.ijheatmasstransfer.2019.04.077

Yoboué, K. E., Bongoua-Devisme, A. J., Kouadio, K. P., & Yao-Kouame, A. (2014). Minéralogie de la fraction argileuse des sols brunifiés de Kahankro et Anikro (Toumodi) dans le Centre Sud de la Côte d'Ivoire. *International Journal of Biological and Chemical Sciences*, *8*(3), 1269. https://doi.org/10.4314/ijbcs.v8i3.40